EBioMedicine 51 (2020) 102596

Contents lists available at ScienceDirect

EBioMedicine

journal homepage: www.elsevier.com/locate/ebiom

Research paper

SH3BGRL2 inhibits growth and metastasis in clear cell renal cell carcinoma via activating hippo/TEAD1-Twist1 pathway

Lei Yin[a,1], Wenjia Li[b,1], Aiming Xu[c], Heng Shi[a], Keyi Wang[a], Huan Yang[d,*], Ronghao Wang[e,*], Bo Peng[a,*]

[a] Department of Urology, Shanghai Tenth People's Hospital, School of Medicine in Tongji University, Shanghai, China
[b] Shanghai Institute of Cardiovascular Disease, Zhongshan Hospital, Fudan University, Shanghai, China
[c] Department of Urology, The First Affiliated Hospital of Nanjing Medical University, Nanjing, China
[d] Department of Urology, Tongji Hospital, Tongji Medical College, Huazhong University of Science and Technology, Wuhan, China
[e] School of basic medical sciences, Southwest Medical University, Luzhou, China

ARTICLE INFO

Article History:
Received 23 October 2019
Revised 6 December 2019
Accepted 6 December 2019
Available online 6 January 2020

Keywords:
Clear cell renal cell carcinoma
SH3BGRL2
Metastasis
Hippo
Twist1

ABSTRACT

Background: Clear cell renal cell carcinoma (ccRCC) is one of the most prevalent malignancies in the world, and tumor metastasis is still the main reason for disease progression. Accumulating evidence shows that SH3BGRL2 may play a key role in tumor progression and metastasis. However, the role of SH3BGRL2 in ccRCC has not been systematically investigated and remains elusive.
Methods: The clinical significance of SH3BGRL2 was evaluated by bioinformatic analysis and tissue microarray (TMA) samples. SH3BGRL2 expression was determined by RT-PCR, western blot and immunohistochemistry staining. Tumor suppressive effect of SH3BGRL2 was determined by both in vitro and in vivo studies. Western blot, chromatin immunoprecipitation assay and luciferase report assay were applied for mechanism dissection.
Findings: SH3BGRL2 was crucial for epithelial-mesenchymal transition (EMT) progression and metastasis in ccRCC. Clinically, SH3BGRL2 was identified as an independent prognostic factor for ccRCC patients. Gain- and loss-of-function results suggested that SH3BGRL2 played a critical role in cell proliferation, migration and invasion. Mechanistically, we found that SH3BGRL2 acted as a tumor suppressor through Hippo/TEAD1 signaling, then TEAD1 altered Twist1 expression at the transcriptional level via directly binding to its promoter region.
Interpretation: Our findings established that SH3BGRL2 performed as a tumor suppressor and modulator via Hippo/TEAD1-Twist1 signaling in ccRCC, and the alteration of SH3BGRL2 could serve as a functional response biomarker of tumor progression and metastasis in ccRCC.

1. Introduction

Renal cell carcinoma (RCC) is one of the most common cancers in the world, accounting for 4.2% of all new cancer cases [1]. Clear cell renal cell carcinoma(ccRCC), which also known as kidney renal clear cell carcinoma (KIRC), is the most common subtype of RCC and accounts for 80% of all kidney cancers [2]. Although several treatments may be beneficial for patients with localized ccRCC, but tumor metastasis is still the main reason for disease progression, and about 30% of patients will relapse after initially surgical resection [3, 4]. Therefore, exploring new molecules involved in ccRCC progression and metastasis is the key to finding new targets for ccRCC treatment.

SH3BGRL2, was first identified in 2002, belong to SH3BGR family, which includes SH3BGR, SH3BGRL, SH3BGRL2 and SH3BGRL3 [5]. Recent study found the expression of SH3BGR family varies significantly at different developmental stages and organ types, suggesting that abnormal expression of SH3BGR members may lead to a variety of diseases [6]. However, biological functions of SH3BGR family members are still largely unclear. Previous study reported SH3BGR suppresses cell migration and angiogenesis in Kaposi's Sarcoma [7]. Interesting, Wang et al. suggested SH3BGRL may be an oncogene in mice, but as a tumor suppressor gene in human [8]. Xu et al. found SH3BGRL as a novel prognostic biomarker is down-regulated in acute myeloid leukemia [9]. Our previous study and another group also found SH3BGRL3 could be as a biomarker in kidney and bladder

Abbreviations: *ccRCC*, Clear Cell Renal Cell Carcinoma; KIRC, Kidney Renal Clear Cell Carcinoma; TMA, Tissue Microarray; CHIP, Chromatin Immunoprecipitation Assay; IVIS, In Vivo Imaging System; ROC, Receiver Operating Characteristic; TCGA, The Cancer Genome Atlas; PDX, Patient-Derived Xenograft

* Corresponding authors.
E-mail addresses: yhpz123@163.com (H. Yang), gmack@163.com (R. Wang), pengbo6908@163.com (B. Peng).
[1] These authors contributed equally to the study

https://doi.org/10.1016/j.ebiom.2019.12.005

Research in context

Evidence before this study

Emerging studies found the expression of SH3BGR family varies significantly at different developmental stages and organ types, suggesting that abnormal expression of SH3BGR members may lead to a variety of diseases. Recently, our study and another study showed that SH3BGRL3 promotes kidney cancer and bladder cancer progression. However, as a novel gene in SH3BGR family, the function of SH3BGRL2 is still largely unknown in clear cell renal cell carcinoma (ccRCC).

Added value of this study

Our findings revealed for the first time that SH3BGRL2 downregulation was commonly detected in high-grade ccRCC and might serve as a biomarker or even a therapeutic target for ccRCC patients. Additionally, gain- and loss-of-function results suggested that SH3BGRL2 played a critical role in ccRCC tumor growth and metastasis. Mechanistically, we found that SH3BGRL2 acted as a tumor suppressor through Hippo/TEAD1/Twist1 signaling pathway.

Implications of all the available evidence

Our findings identified SH3BGRL2 as a novel tumor suppressor gene that modulates the metastatic potentials of ccRCC, and suggested that SH3BGRL2 servered as a clinical biomarker and SH3BGRL2/ Hippo/TEAD1/ Twist1 signaling pathway might be a promising therapeutic target for ccRCC.

cancer [10, 11]. SH3BGRL2, as a new member of the SH3BGR family, containing a Src homology 3 (SH3) and an ENA/VASP Homology 1 (EVH1) domain, located in the nucleus and in the perinuclear region [5]. Considerable evidence suggests that SH3 and EVH1 domain plays a central role in cell growth, adhesion and migration [12, 13], indicate SH3BRGL2 may involve in a variety of biological procession. Tong et al. reported that SH3BGRL2 might play a crucial role in nervous system development and intestine formation in zebrafish model [6]. Recently, emerging studies reported SH3BGRL2 were significantly down-regulated in esophageal squamous cell carcinoma [14] and ovarian cancer [15], which meant SH3BGRL2 might play a key role in tumor suppression. However, the detailed function of SH3BRGL2 in tumor, especially in ccRCC, remains elusive.

Hippo pathway is a highly conserved signaling pathway, which mainly comprises large tumor suppressor 1/2 (LATS1/2), yes association protein (YAP) and TEA domain (TEAD) transcription factors [16]. Decreased LATS1/2 expression contributed to many types of tumor progression, such as colorectal cancer and lung cancer [17, 18]. Our previous study also found loss of LATS1/2 are correlated with poor survival in RCC patients [19]. Once hippo signaling is activated, YAP is phosphorylated and then degraded in the cytoplasm. But when YAP is activated, it localizes in the nucleus and binds to TEAD, then drives tumor growth and metastasis [20]. Moreover, YAP could also promote tumor angiogenesis and dasatinib resistance in renal cell carcinoma [21, 22]. However, whether YAP promotes ccRCC metastasis remains unclear.

In this study, we first investigated the biological mechanism of SH3BGRL2 in ccRCC. Surprisingly, we found that the expression of SH3BGRL2 was significantly reduced in tumor tissues and cells, and its low expression predicted a poor prognosis in patients with ccRCC. Subsequently, our gain- and loss-of-function experiments indicated SH3BGRL2 significantly inhibited proliferation, migration and invasion of tumor cells. Further studies found that SH3BGRL2 could inhibit the metastasis of ccRCC by regulating Hippo/TEAD1 signaling pathway, then TEAD1 altered Twist1 expression at the transcriptional level via directly binding to its promoter region. Collectively, our results indicated SH3BGRL2 might serve as a biomarker in judging the tumor progression and as a new target for ccRCC treatment.

2. Materials and methods

2.1. Clinical tissues

Three independent cohorts of ccRCC surgical specimens were obtained from Shanghai Tenth People's Hospital. For group 1, tissue microarrays (TMAs), 112 ccRCC and 30 adjacent non-tumor tissues were collected. For group 2, 16 fresh clinical samples were collected for further PCR, western blot (WB) and Immunohistochemistry (IHC) detection. For group 3, 5 patients suffered recurrence were enrolled. Their matched adjacent normal tissues, primary tumor, and recurrent tumor tissues were collected for further WB assay. The tissue samples used for the study were conformed to the 1975 Declaration of Helsinki and was approved by the ethics committee of Shanghai Tenth People's Hospital, School of Medicine in Tongji University. Informed consent was obtained from all patients.

2.2. Cell culture and lentivirus transfection

HK2, A498, 769-P, ACHN, 786-O, Caki-1and Caki-2 were obtained from Cell Bank of the Chinese Academy of Sciences. HK2 cells were cultured in Keratinocyte Serum Free Medium and the other tumor cell lines were cultured in Dulbecco's modified Eagle's medium. All cells were supplemented with 10% fetal bovine serum, 1% penicillin/streptomycin and cultured in humidified chamber at 37 °C under 5% CO^2. The lentivirus packaging were using 239T cells. Briefly speaking, the pLKO.1 and pWPI plasmids were used as vector, psPAX2 and pMD2.G were used as packaging and envelop plasmids. The target sequences used in this study are listed in Supplemental Information, Methods and Materials.

2.3. Western blot

Western blot assay were performed as described previously [23]. Briefly speaking, cells were lysed in RIPA lysis buffer containing PMSF on ice. The concentrations of proteins were determined using a BCA protein kit (Beyotime, China) and whole lysates were mixed with 6 × SDS loading buffer, heated at 100 °C for 10 min. A total of 30 μg of protein from each sample were loaded, running and then transferred to PVDF membranes. Immunoreactive bands were visualized using ECL western blot kit. The detailed antibodies are listed in Supplemental Information, methods and materials.

2.4. RNA extraction and quantitative real-time PCR

Total RNA was extracted using an RNeasy mini kit (Qiagen, Germany). The RNA concentration was measured using Nanodrop 2000 (Thermo Scientific, USA). cDNA was synthesized using the QuantiTect Reverse Transcription Kit (Qiagen) with the primers (Sangon Biotech, Shanghai, China) according to the manufacturer's instructions. GAPDH was used to correct the difference in template input. The relative RNA expression was calculated using the $2^{-\Delta CT}$ method. The detailed primers are listed in Supplemental Information, Methods and Materials.

2.5. Cell proliferation, colony formation, wound healing and Matrigel invasion assays

Cell proliferation was measured by CCK-8 Kit according to the manufacturer's protocols. For colony formation assay, cells were seeded in 6-well plates at a density of 5 × 10^2 cells per well then

stained and photographed after 2 weeks. Wound healing assay were used to detect cell migration ability as previously describe [24]. Cell invasion assay were performed using matrigel-coated chamber (Corning, USA). In brief, 5×10^4 ccRCC cells with serum-free media were seeded into the upper chambers and stained after 24 h.

2.6. Tissue microarray and immunohistochemistry

The production of tissue microarray (TMA) was as described previously [25]. Briefly, a 0.6 mm diameter cylinder was used to take the core from the representative area of each tissue and the tissue cylinder was placed in a paraffin block. Immunohistochemistry (IHC) experiments were performed as previously described [26]. In general, tissue sections were incubated with primary antibodies and placed at 4 °C overnight, then secondary antibodies were incubated at room temperature. IHC staining was independently assessed by three experienced pathologists. The immunoreactive score representing the proportion of positively stained tumor cells were graded as: 0 (<10%); 1 (11%–25%); 2 (26%–50%); 3 (51%–75%) and 4 (>75%). The intensity of staining was determined as: 0 (no staining); 1 (weak staining = light yellow); 2 (moderate staining = yellow brown); and 3 (strong staining = brown). A semiquantitative scoring criterion was used, in which the staining index (values 0–12) were calculated by multiplying the staining intensity and the positive cells proportion. Finally, cases were classified into two different groups: low expression cases (score 0–6) and cases with high expression (score 7–12).

2.7. Chromatin immunoprecipitation assay

The CHIP assay were in accordance with the Cold Spring Harbor protocol [27]. Briefly speaking, cells were treated with 1% formaldehyde at room temperature for 10 min to cross-link DNA. After sonication, cross-linked chromatin was pre-cleared with A/G-agarose beads, then immunoprecipitated with anti-TEAD1 antibody overnight at 4 °C. For the negative control, IgG was used. Specific primers for amplifying the target sequence of the human Twist1 promoter are listed in Supplemental Information, Methods and Materials. PCR products were identified by agarose gel electrophoresis.

2.8. Luciferase reporter assay

Human Twist1 promoter region was constructed into pGL3-basic vector (Promaga, USA). Then cells were seeded in 24-well plates and transfected with cDNA via Lipofectamine 3000 (Invitrogen). pRL-TK was used as negative control. The luciferase activity measured were based on the manufacturer's manual (Promega).

2.9. Xenograft tumor and metastasis assay

The animal experiment was approved by the animal committee of Tongji university. For tumor growth model, 2×10^6 cells with Luciferase reporter were injected subcutaneously into the flanks of nude mice. The tumor growth was measured every week and mice were sacrificed four weeks later. The tumor volume was calculated by length $\times$ width$^2 \times 0.5$. To generate tumor metastasis model, 2×10^6 cells were suspended in 100μl of PBS and injected into the tail vein of nude mice. Metastases were monitored through IVIS Lumina II system (Caliper Life Sciences, Hopkinton, MA). The bilateral lung tissues were excised and photoed, then fixed with 4% paraformaldehyde at room temperature and analyzed by HE staining. Mouse survival was monitored after tumor transplantation.

2.10. Statistical analysis

Statistical analysis was performed using SPSS 23.0 software (IBM, USA). For comparisons, the Chi-square ($\chi 2$), Student's *t*-test and One way ANOVA were used, as appropriate. The optimal cut-off value was determined by a ROC curve analysis in MedCalc software (MedCalc, Korea). Survival curves were calculated using the Kaplan-Meier method and differences were assessed by log-rank test. The Cox proportional hazards model was used to determine risk factors, which were screened by univariate analysis. Statistical significance was indicated by p values $^*p < 0.05$, $^{**}p < 0.01$ and $^{***}p < 0.001$.

3. Results

3.1. The pattern and significance of SH3BGRL2 in TCGA

To determine the role of SH3BGRL2 in ccRCC, we firstly detected the expression level of SH3BGRL2 in TCGA and GEO database. Interestingly, SH3BGRL2 was downregulated in tumor tissues compared with normal kidney tissues from TCGA database (Fig. 1a left). In addition, decreasing of SH3BGRL2 was observed in ccRCC metastatic-PDX tissues when compared with primary-PDX tissues (Fig. 1a right). Subsequently, the TCGA data showed that patients with lower expression levels of SH3BGRL2 had worse survival (Fig. 1b) and shorter disease-free survival rate (Fig. 1c). Furthermore, statistical analysis revealed that SH3BGRL2 expression was correlated with TNM stage (Fig. 1d-f), pathology histologic grade (Fig. 1g), clinical stage (Fig. 1h) and tumor recurrence (Fig. 1i) in TCGA patients (Supplementary Table 1), and 3 studies in Oncomine (www.oncomine.org) also confirmed these findings (Supplementary Fig. 1a-h). Besides, we also found the expression level of SH3BGRL2 in ccA subtype was higher than ccB subtype(Supplementary Fig. 2), which suggested a better long-term prognosis [28]. More importantly, according to the pathological grade and clinical stage classification, patients in each stage or grade with SH3BGRL2 low expression had poorer survival with those with SH3BGRL2 high expression (Supplementary Fig. 3a-h).

To evaluate whether the expression levels of SH3BGRL2 was associated with prognosis of ccRCC patients, based on the optimal cut-off values of SH3BGRL2 (Supplementary Fig. 4a-b), the 533 ccRCC patients were divided into two groups: SH3BGRL2 high expression group and SH3BGRL2 low expression group (Supplementary Table 1). Univariate Cox proportional hazards regression analysis showed that advanced TNM stage, pathological grade, clinical stage, recurrence status and low expression of SH3BGRL2 were correlated with poorer overall survival (Fig. 1j, Supplementary Table 2). In addition, the multivariate Cox regression analysis revealed SH3BGRL2, combined with tumor metastasis and advanced clinical grade stage, were independent prognostic factors for ccRCC patients (Fig. 1k, Supplementary Table 2). These data suggested that SH3BGRL2 played a vital role in tumor progression and metastasis in ccRCC.

Moreover, analysis of TCGA database showed that SH3BGRL2 was significantly decreased in various types of human cancer, such as breast, uterus, esophagus, brain, blood, lung and skin cancer (Supplementary Fig.5a), and SH3BGRL2 down regulation correlated with poor prognosis in human cancers, including ovarian cancer, thyroid carcinoma, pheochromocytoma and paraganglioma, lung adenocarcinoma, head-neck squamous cell carcinoma and breast cancer(Supplementary Fig.5b), which indicated that SH3BGRL2 might be a critical tumor suppressor gene in various tumors.

3.2. Dysregulated SH3BGRL2 in ccRCC indicates a poor prognosis

Considering the SH3BGRL2 expression level in TCGA database was detected by RNA sequencing. Thus, we analyzed a large cohort of clinical samples both in RNA and protein level to verify the results in TCGA database. Consistently, SH3BGRL2 expression was lower in 62.5% ccRCC patients than paired adjacent normal tissues (Fig. 2a). WB assays also confirmed the RT-PCR findings (Fig. 2b). Moreover, the expression levels of SH3BGRL2 showed a decreasing trend in matched adjacent non-tumor tissue, primary tumor, and recurrence

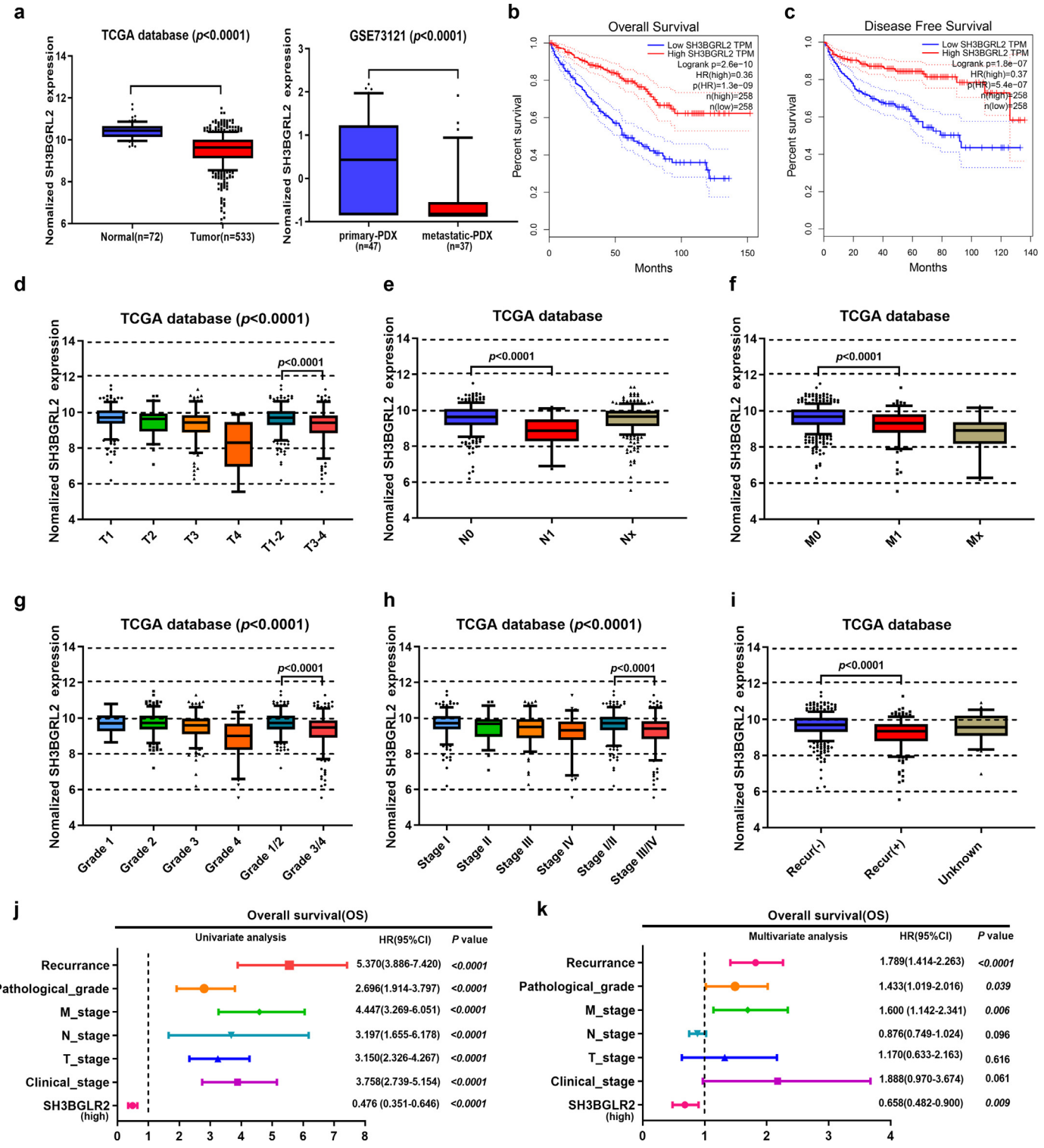

Fig. 1. The Pattern and Significance of SH3BGRL2 in TCGA. a. The expression of SH3BGRL2 in ccRCC from TCGA database(**left**) and GEO database(**right**). **b-c.** Kaplan–Meier analysis indicated that higher expression of SH3BGRL2 was associated with longer overall survival(**b**) and disease-free survival(**c**). **d-i.** The expression of SH3BGRL2 in different grades and stages: tumor stage(**d**), lymphatic invasion(**e**), metastasis status(**f**), pathological grade(**g**), clinical stage(**h**), recurrence status(**i**). **j-k.** The outcomes of univariate(**j**) and multivariate(**k**) analysis. The HRs are presented as the means (95% confidence interval). The n values indicate the number of patients. Error bars represent SD of the mean. (Student's *t*-test, one-way ANOVA).

samples from 5 recurrent patients (Fig. 2c), which consistent with TCGA analysis results.

Next, the correlation between SH3BGRL2 and ccRCC prognosis was evaluated. Immunohistochemistry (IHC) staining showed SH3BGRL2 expression was shrinking continuously in clinical Fuhrman stage (Fig. 2d and 2f), and also downregulated in 112 ccRCC tissues compared with 30 normal kidney tissues (Fig. 2e). Moreover, patients with lower SH3BGRL2 expression were correlated with the advanced tumor stage (Fig. 2g, Table 1) and metastasis status (Fig. 2h, Table 1). Kaplan–Meier analysis showed that the 5-year overall survival rate for ccRCC patients with lower SH3BGRL2 expression significantly reduced when compared with the patients with higher

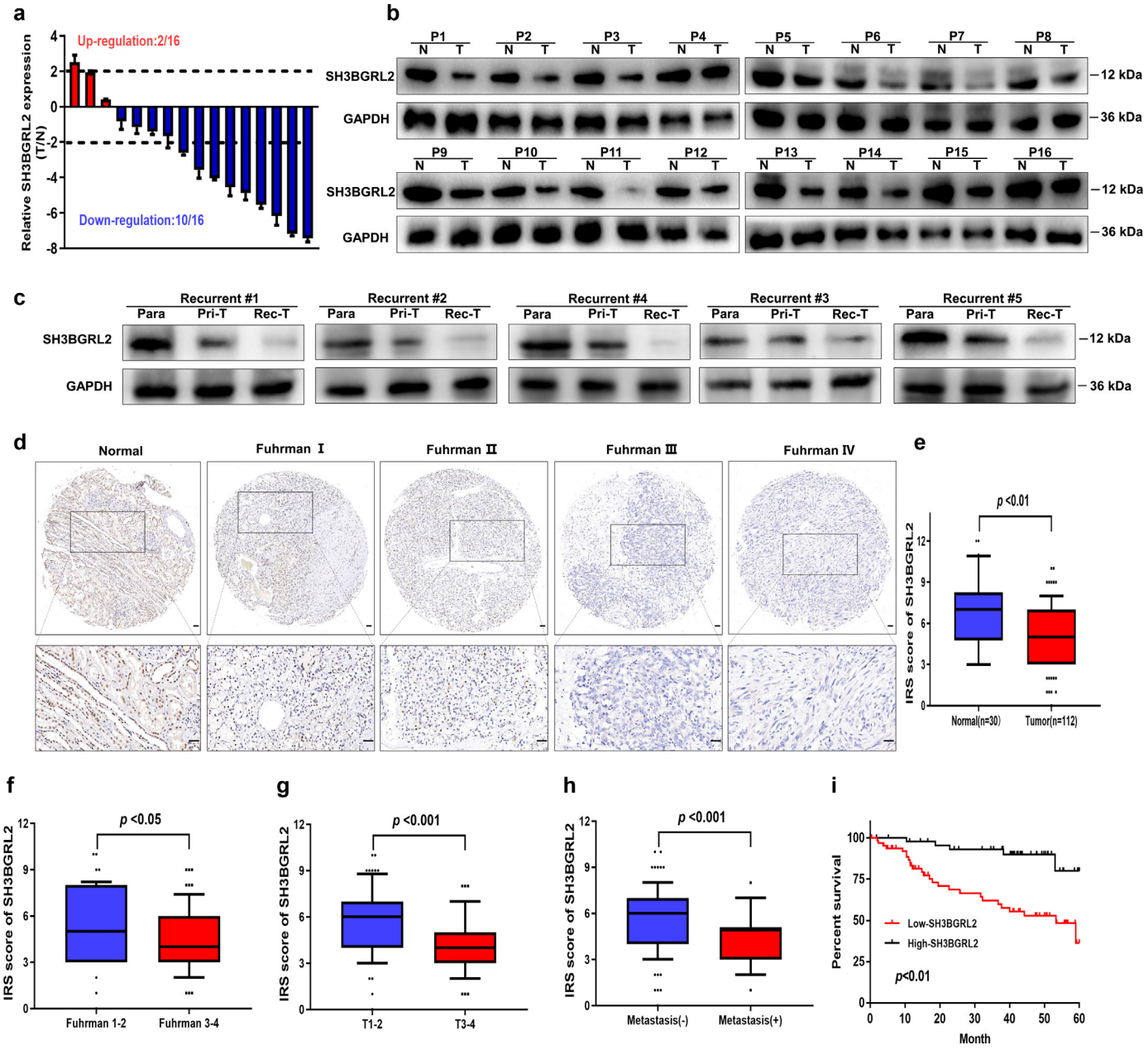

Fig. 2. Dysregulated SH3BGRL2 in ccRCC indicates a poor prognosis. a-b. RT-PCR(**a**) and western blot(**b**) analysis of SH3BGRL2 expression levels in 16 ccRCC tissues and paired non-tumor kidney tissues. **c.** Western blot analysis of SH3BGRL2 expression in matched para-tumor, primary-tumor and recurrent tumor tissues. **d-e.** Representative TMA images show SH3BGRL2 staining(**d**), and comparison of the IHC score between tumor and non-tumor kidney tissues(**e**). **f-h.** The expression of SH3BGRL2 in different grades and stages: fuhrman grade(**f**), tumor stage(**g**) and metastasis status(**h**). **i.** Kaplan–Meier analysis of TMA patients with low versus high expression levels of SH3BGRL2. The n values indicate the number of patients. Error bars represent SD of the mean.

SH3BGRL2 expression (Fig. 2i). More importantly, expression of SH3BGRL2 was correlated with OS (p = 0.031, hazard ratio (HR)= 0.329, Table 2), which was consistent with our previously TCGA results (Fig. 1k and 1l).

Taken together, combined public RNA-seq data with our clinical data, these findings indicated that downregulation of SH3BGRL2 might play a potential role to promote the malignant progression of ccRCC.

3.3. SH3BGRL2 inhibited proliferation, migration and invasion of ccRCC cells

Next, the biological functions of SH3BGRL2 in ccRCC progression were investigated. In order to choose the most suitable RCC cell lines, we detected SH3BGRL2 expression level in human renal proximal tubular epithelial cells HK2, clear cell renal cell carcinoma (ccRCC) line A498, 769-P, 786-O, Caki-1 and papillary renal cell carcinoma (pRCC) cell lines ACHN, Caki-2. Real-time PCR and western blot showed that SH3BGRL2 mRNA and protein expression, respectively, were markedly downregulated in all RCC cell lines compared to primary normal HK2 cells (Fig. 3a and 3b). At last, we chose to establish SH3BGRL2 stable knockdown (choose the high efficiency SH1) in 786-O (Fig. 3c left, which has more endogenous SH3BGRL2) and overexpression in A498 cell lines (Fig. 3c right, which has less endogenous SH3BGRL2). Strikingly, CCK-8 assay showed SH3BGRL2 depletion enhanced 786-O cell line proliferation (Fig. 3d left), and SH3BGRL2 overexpression reduced it in A498 cell line (Fig. 3d right). The colony formation assay also demonstrated these findings (Fig. 3e and 3f). Results of both wound-healing assay and transwell assay revealed that the 786-O sh-SH3BGRL2

Table 1
Correlation between clinic-pathological parameters of patients enrolled.

Clinical characteristics	No.of patients (n = 112)	SH3BGRL2 low (n = 64)	SH3BGRL2 high (n = 48)	P value[a]
Age (years)				0.544
≤60	64	35	29	
>60	48	29	19	
Gender				0.134
Male	74	46	28	
Female	38	18	20	
Tumor size				0.784
≤4 cm	52	29	23	
>4 cm	60	35	25	
Laterality				0.091
Left	55	27	28	
Right	57	37	20	
Fuhrman grade				0.269
G1-2	47	24	23	
G3-4	65	40	25	
T stage				***0.001****
Ⅰ-Ⅱ	71	32	39	
Ⅲ-Ⅵ	41	32	9	
Metastasis				***0.019****
No	94	52	42	
Yes	18	4	14	

* Statistically significant ($p < 0.05$).
[a] p value from Chi-square test.

cells had a higher wound-closure rate and more capacity of cell invasions than mock control cells(Fig. 3g and 3i), whereas the A498 OE-SH3BGRL2 cells had a slower migratory and less invasive capacity than vector control cells(Fig. 3h and 3j). Therefore, our in vitro data showed SH3BGRL2 played a suppressive role in regulation of proliferation, migration, and invasion in ccRCC cells.

3.4. SH3BGRL2 suppressed the growth and metastasis of ccRCC cells in vivo

The above data demonstrated that SH3BGRL2 might acted as a tumor suppressor gene to deplete ccRCC cell proliferation, migration and invasion. We next explored SH3BGRL2 function in vivo. The 786-O/sh-SH3BGRL2 cells were inoculated into the flank of nude mice. As In Vivo Imaging Systems (IVIS) showed, SH3BGRL2 knocked-down significantly promoted tumor proliferation (Fig. 4a), evidenced by larger tumor volume (Fig. 4b) and heavier tumor weight (Fig. 4c).

To further explore the effects of SH3BGRL2 in tumor metastasis, 786-O cells labeled with luciferase were injected into tail vein of nude mice. Increased luciferase signal in tumors of the sh-SH3BGRL2 group was detected by the IVIS, showing SH3BGRL2 knocked-down promoted ccRCC cell metastases (Fig. 4d). HE analysis also showed an increase of pulmonary nodules metastasis in sh-SH3BGRL2 group compared with control group (Fig. 4e and 4f). Consistently, metastatic foci volume of the sh-SH3BGRL2 group in lung and liver were larger than the control group (Fig. 4g and 4h), and more lung and liver metastases occurred in sh-SH3BGRL2 group (Fig. 4i and 4j). More importantly, SH3BGRL2 knocked-down impaired mouse survival (Fig. 4k). Collectively, these observations demonstrated that inhibition of SH3BGRL2 might promote the growth and metastasis of ccRCC cells in vivo.

Table 2
Univariate and multivariate cox proportional regression analysis with overall survival.

	Univariate analysis		Multivariate analysis	
	HR (95%CI)	P value	HR (95%CI)	P value
Age (years)				
≤60	1.000	***0.012****	1.000	***0.020****
>60	2.550(1.229−5.290)		2.500(1.152−5.423)	
SH3BGRL2				
Low	1.000	***0.001****	1.000	***0.031****
High	0.195(0.075−0.510)		0.329(0.119−0.905)	
Gender				
Female	1.000	0.536	NA	
Male	0.782(0.360−1.701)			
Tumor size				
≤4cm	1.000	0.430	NA	
>4cm	1.338(0.649−2.761)			
Laterality				
Left	1.000	0.283	NA	
Right	0.675(0.330−1.383)			
Fuhrman grade				
G1-2	1.000	***0.002****	1.000	0.335
G3-4	4.598(1.756−12.036)		1.769(0.554−5.645)	
T stage				
Ⅰ-Ⅱ	1.000	<***0.0001****	1.000	0.286
Ⅲ-Ⅵ	6.134(2.730−13.784)		1.714(0.637−4.610)	
Metastasis				
No	1.000	<***0.0001****	1.000	***0.001****
Yes	7.739(3.743−16.000)		4.233(1.766−10.148)	

CI confidence interval, HR hazard ratio.
* Statistically significant ($p < 0.05$)
p value from Cox regression analyses.

3.5. SH3BGRL2 inhibited epithelial−mesenchymal transition (EMT) of ccRCC cells

To dissect the detailed mechanism of SH3BGRL2, we analyzed the ccRCC RNA expression profiles from TCGA database. Interestingly, GO enrichment showed that SH3BGRL2 might participate in membrane related processes, such as hippo signaling, cell junction and endothelium development (Fig. 5a; Supplementary Fig. 6a-f; Table S3). Gene set enrichment analysis (GSEA) showed SH3BGRL2 expression was significantly positive with renal system process (Fig. 5b) and cell-cell junction (Fig. 5c), which means SH3BGRL2 might paly pivotal role in renal system and tumor EMT progression.

Previous studies reported that most of ccRCC were derived from renal tubular epithelial cells, and epithelial-mesenchyme transition (EMT), is a key event that occurs during the cancer invasion and metastasis with epithelial origin [29, 30]. Based on this, the expression of EMT markers was detected both in mRNA and protein level. The results indicated that ZO-1 and E-cadherin, which epithelial marker, were decreased, whereas the levels of mesenchymal markers including N-cadherin, Vimentin and Twist1 were all increased in 786-O sh-SH3BGRL2 cells (Fig. 5d and f). Conversely, upregulated of SH3BGRL2 in A498 cells led to upregulation of ZO-1 and E-cadherin but downregulation of N-cadherin, Vimentin and Twist1 (Fig. 5e and g). The immunofluorescence assay also confirmed these results (Fig. 5h). Therefore, SH3BGRL2 acted as a suppressor of EMT in ccRCC cells.

3.6. SH3BGRL2 regulated ccRCC cell proliferation and EMT via Hippo signaling pathway

Hippo signaling pathway plays a vital role in many physiological processes including cell proliferation, differentiation, survival and metastasis [19, 31, 32]. Moreover, GO enrichment (Fig. 5a) and GSEA analysis (Fig. 6a) showed SH3BGRL2 expression was positively with hippo signaling pathway. The pathway enrichment analysis by GeneMANIA [33] also showed that the hippo signaling pathway was significantly enriched with SH3BGRL2 (Fig. 6b). Additionally, SH3BGRL2 expression was positively correlated with LATS1 and LATS2 expression in TCGA database (Fig. 6c-d). Therefore, we wondered whether SH3BGRL2 functioned in ccRCC through regulating hippo signaling pathway. As expected, western blot showed that LATS1, LATS2 and phosphorylation of YAP were significantly downregulated in 786-O sh-SH3BGRL2 cells (Fig. 6e). Conversely, upregulating SH3BGRL2 in A498 cells led to upregulation of LATS1, LATS2 and phosphorylation of YAP (Fig. 6f). Previous study indicated when hippo signaling activated, YAP would be phosphorylated and then degraded in the cytoplasm. But when YAP actived, it would localize to the nucleus and binds to TEAD, then drives tumor growth and metastasis [20].

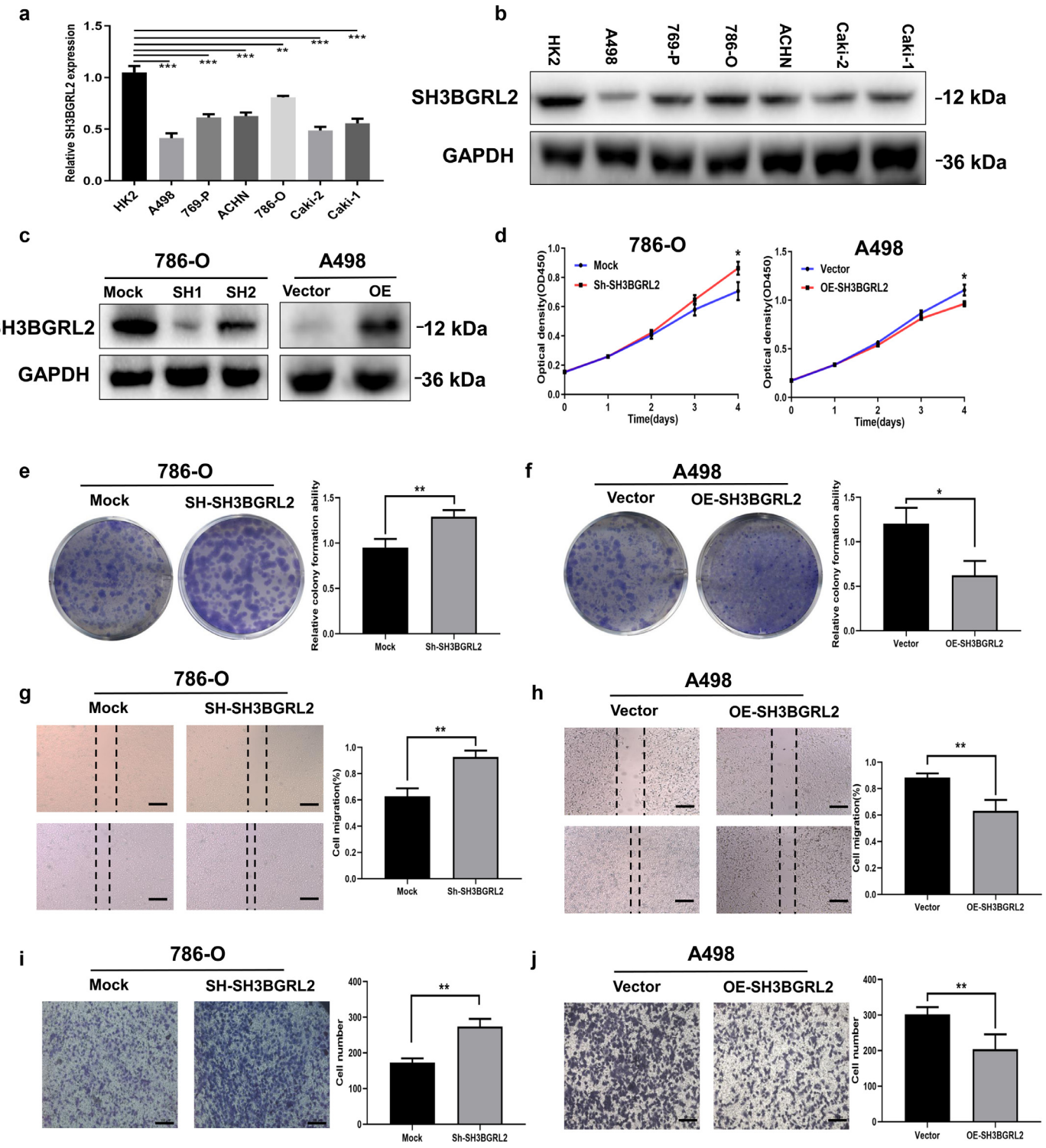

Fig. 3. SH3BGRL2 inhibited proliferation, migration and invasion of ccRCC cells. a-b. RT-PCR(**a**) and western blot(**b**) analysis of SH3BGRL2 expression levels in different RCC cell lines and normal HK2 cell line. **c.** Western blot assays validating the efficiencies of SH3BGRL2 knockdown in 786-O cells (**left**) and overexpression in A498 cells (**right**). **d.** CCK-8 assay analyzing cell proliferation in 786-O cells (**left**) and A498 cells (**right**). **e-f.** Colony formation assay assessing cell proliferative ability in 786-O cells (**e**) and A498 cells (**f**). **g-h.** Cell migratory ability was assessed by wound healing assay in 786-O cells (**g**) and A498 cells(**h**). **i-j.** Transwell assay assessing cell invasion ability in 786-O cells (**i**) and A498 cells (**j**). Data are given as mean ± SD.$^{*}P < 0.05$, $^{**}P < 0.01$, $^{***}P < 0.001$ (Student's *t*-test).

Consistent with those studies, SH3BGRL2 knockdown promoted (Fig. 6g and 6h) and overexpression of SH3BGRL2 inhibited (Fig. 6i and 6j) nuclear translocation of YAP and TEAD1 enrichment. Furthermore, LATS1 and LATS2 were significantly decreased in metastasis ccRCC (Fig. 6k and 6n), advanced pathological grade (Fig. 6i and 6o) and clinical stage (Fig. 6m and 6p) in TCGA database. The Kaplan–Meier analysis also revealed that patients with higher LATS1 or LATS2 expression in ccRCC had significantly long OS and DFS (Supplementary Fig.7a-b).

To illustrate whether hippo signaling pathway was critical for SH3BGRL2 mediated ccRCC cells growth and metastasis, we treated 786-O/sh-SH3BGRL2 and A498/OE-SH3BGRL2 cells with YAP-TEAD1 specific inhibitor Peptide 17 [34] and OE-TEAD1. The results revealed that the Peptide 17 or OE-TEAD1 significantly alleviated

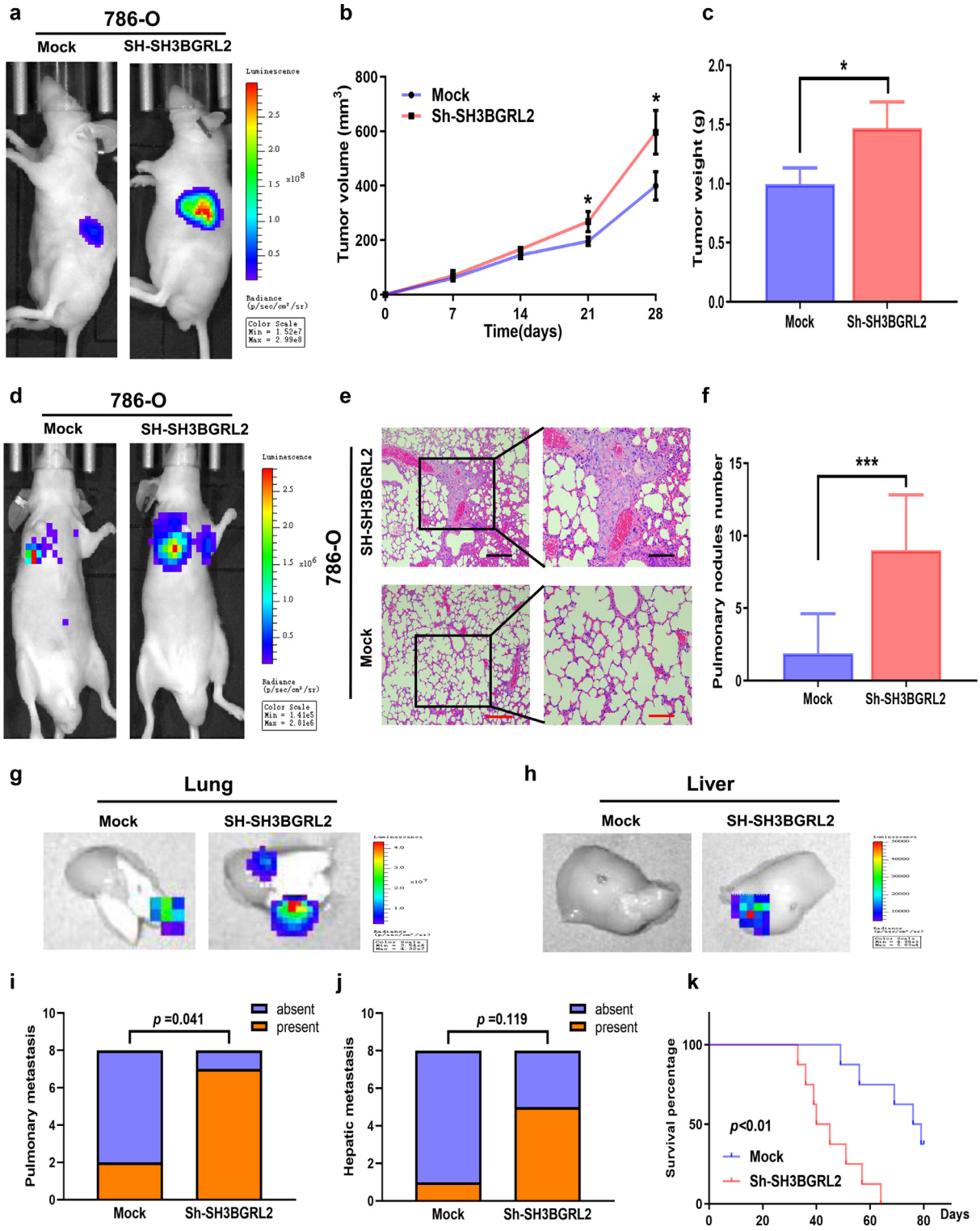

Fig. 4. SH3BGRL2 suppressed the growth and metastasis of ccRCC cells in vivo. a. Representative images of BALB/c nude mice injected with 786-O cells subcutaneously. **b.** Analysis of tumor volume of mice measured every week ($n = 4$ per group). **c.** Analysis of tumor weight of xenograft tumors($n = 4$ per group). **d.** Representative images of metastasis by an in vivo bioluminescence imaging system. **e.** HE images of pulmonary micro-metastases. **f.** the number of pulmonary metastasis in each group. **g-h.** Macroscopic appearance of lung (**g**) and liver(**h**) metastatic nodule. **i-j.** The number of mice with lung(**i**) and liver(**j**) metastases in each group ($n = 8$ per group). **k.** Mice survival curves ($n = 8$ per group). Data are given as mean ± SD.$^{*}P < 0.05$, $^{**}P < 0.01$, $^{***}P < 0.001$ (Student's *t*-test, Chi-square test).

or promoted the effects of SH3BGRL2 on proliferation (Fig. 7a and 7b, Supplementary Fig. 8), migration (Fig. 7c and 7d) and invasion (Fig. 7e and 7f, Supplementary Fig. 9) in ccRCC cells. Meanwhile, western blot assay indicated that the EMT related marker protein level were reversed in 786-O sh-SH3BGRL2 cells treated with Peptide 17(Fig. 7g) and in A498 cells co-transfected with SH3BGRL2 and TEAD1(Fig. 7h). Collectively, these results demonstrated that SH3BGRL2 inhibited the proliferation, migration and invasion abilities of ccRCC cells through activating LATS1/2-YAP-TEAD1 signaling pathway.

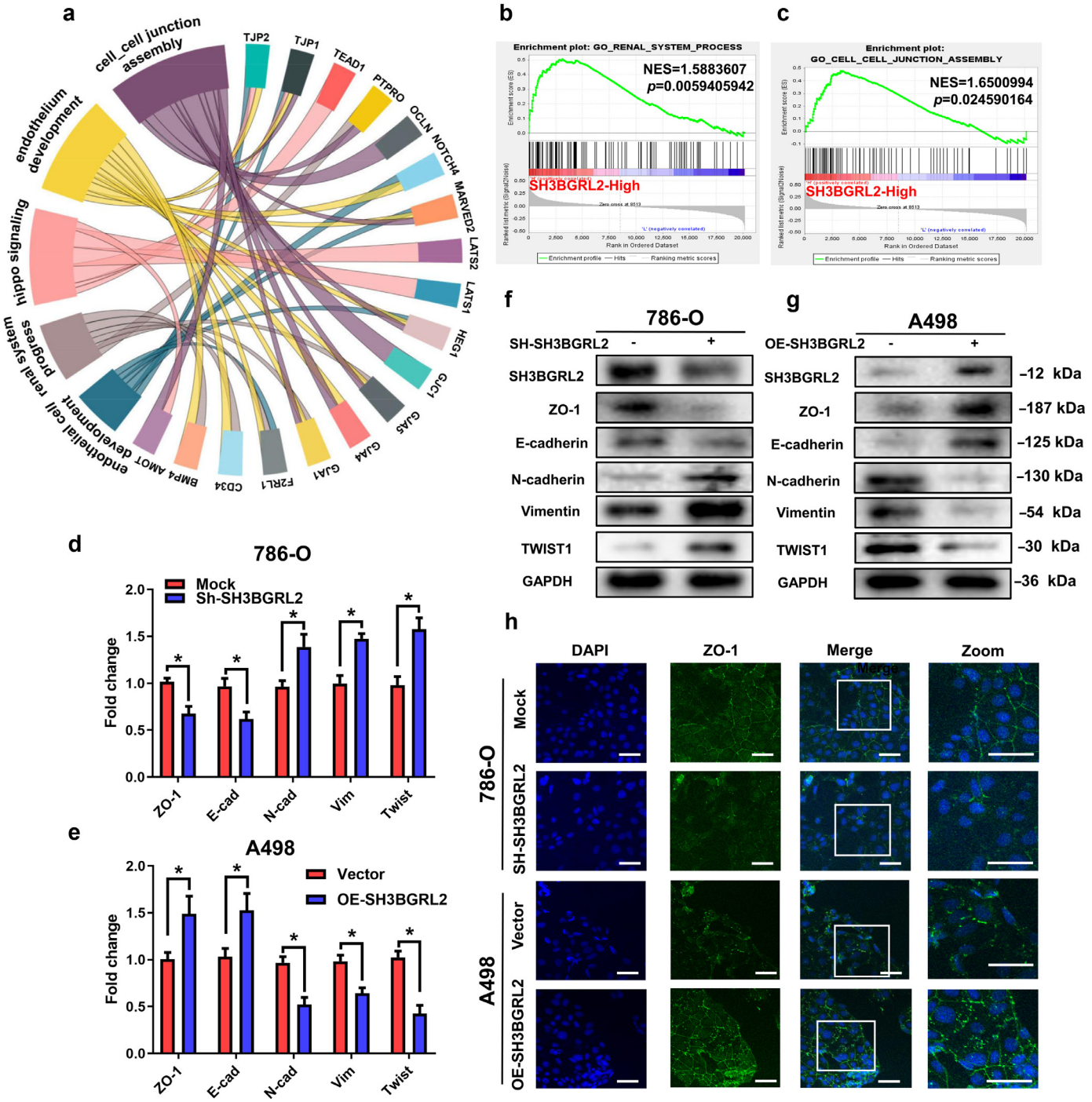

Fig. 5. SH3BGRL2 inhibited epithelial–mesenchymal transition (EMT) of ccRCC cells. a. Chord graph representing 18 differentially expressed genes between SH3BGRL2 high expression group and SH3BGRL2 low expression group and the association of these genes to the corresponding raft-related GO terms. **b-c.** GSEA plot showed SH3BGRL2 level was positively correlated with renal system process(**b**) and cell-cell junction(**c**) in the TCGA dataset. **d-e.** mRNA expression of EMT-related markers were detected in 786-O cells (**d**) and A498 cells (**e**). **f-g.** Protein expression of EMT-related markers were detected in 786-O cells (**f**) and A498 cells (**g**). **h.** Immunofluorescence assays detected ZO-1 expression in 786-O and A498 cells. Data are given as mean ± SD.*$P < 0.05$ (Student's *t*-test).

3.7. TEAD1 promoted EMT by transcriptional up-regulation TWIST1

TEAD1, as a co-transcriptional activator of YAP, mediates YAP-induced cell growth, oncogenic transformation, and EMT in many cancers [35-37]. Our above data indicated SH3BGRL2 inhibited ccRCC cells EMT through YAP-TEAD1 pathway. In addition, we found SH3BGRL2 influence Twist1 expression at the mRNA and protein levels (Fig. 5d-g). In particular, Twist1, as a key regulator in the EMT program [38], were much higher in ccRCC tumor tissues than in adjacent normal tissues(Fig. 8a). Moreover, Twist1 expression was higher in advanced pathological grades (Supplementary Fig. 10a) and clinical stages (Supplementary Fig. 10b). The Kaplan–Meier analysis also revealed that patients with higher Twist1 expression in ccRCC had significantly short OS (Fig. 8b) and DFS (Fig. 8c). Thus, these results suggested that Twist1 is a key factor of EMT in ccRCC and Twist1 might the target gene of the co-transcriptional activators YAP/TEAD1.

To test this hypothesis, we firstly analyzed the Twist1 promoter using JASPAR database [39] to search for potential TEAD1 response

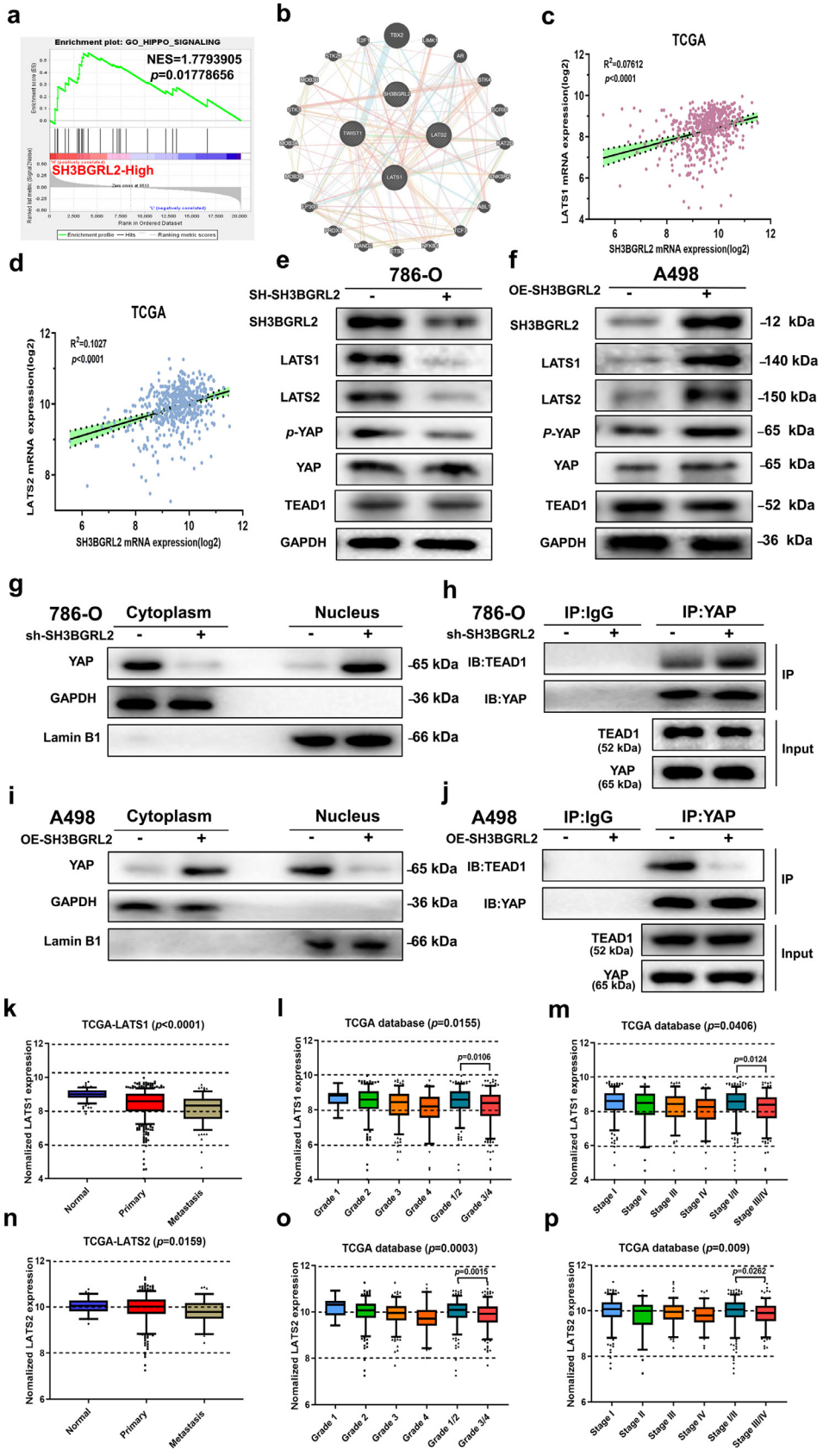

Fig. 6. SH3BGRL2 regulated ccRCC cell proliferation and EMT via Hippo signaling pathway. a. GSEA plot showed SH3BGRL2 level was positively correlated with Hippo signaling pathway in TCGA dataset. **b.** GeneMANIA analysis of SH3BGRL2 regulated hippo pathway genes. **c-d.** TCGA database indicated SH3BGRL2 was positively associated with LATS1(**c**) and LATS2(**d**). **e-f.** The protein expression of LATS1, LATS2, YAP and TEAD1 in 786-O cells (**e**) and A498 cells (**f**). **g, i.** Immunoblotting analysis of YAP in cytoplasm and nucleus in 786-O cells (**g**) and A498 cells (**i**) separately. **h, j.** Co-immunoprecipitation with precipitating YAP or IgG antibodies and immunoblotting with YAP and TEAD1 in 786-O cell (**h**) and A498 cell (**j**). **k, n.** Compared the expression of LATS1(**k**) and LATS2(**n**) in adjacent normal tissue, primary-tumor and metastasis tumor tissues in TCGA database. **i-m.** The expression of LATS1 in different grades(**i**) and stages(**m**) in TCGA database. **o-p.** The expression of LATS2 in different grades(**o**) and stages(**p**) in TCGA database. (Student's *t*-test, one-way ANOVA).

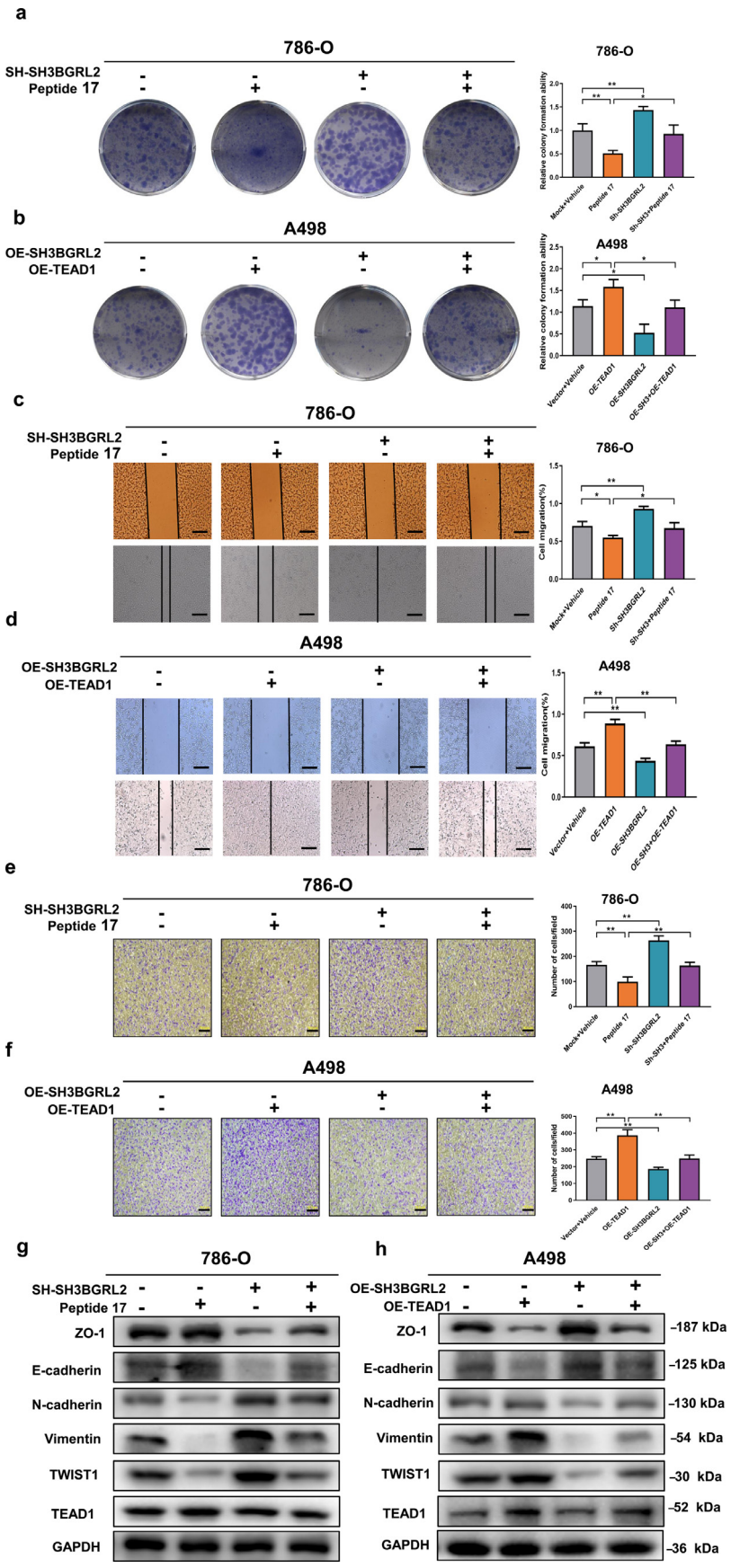

Fig. 7. SH3BGRL2 suppressed ccRCC proliferation, migration and invasion via modulating Hippo signaling. a-f. Colony formation assay(**a, b**), wound healing assay(**c, d**) and transwell assay(**e, f**) usingYAP-TEAD1 specific inhibitor Peptide17 or overexpressing TEAD1 to demonstrate the functional connection of SH3BGRL2 and Hippo signaling pathway in ccRCC cell lines. **g-h.** Western blot demonstrated that inhibit TEAD1 could rescue the EMT progression after knockdown of SH3BGRL2 in 786-O cells(**g**), while promotion of TEAD1 could partially hinder the decreasing of EMT protein levels after overexpressing SH3BGRL2 in A498 cells(**h**). Data are given as mean ± SD.$^{*}P < 0.05$, $^{**}P < 0.01$(Student's *t*-test).

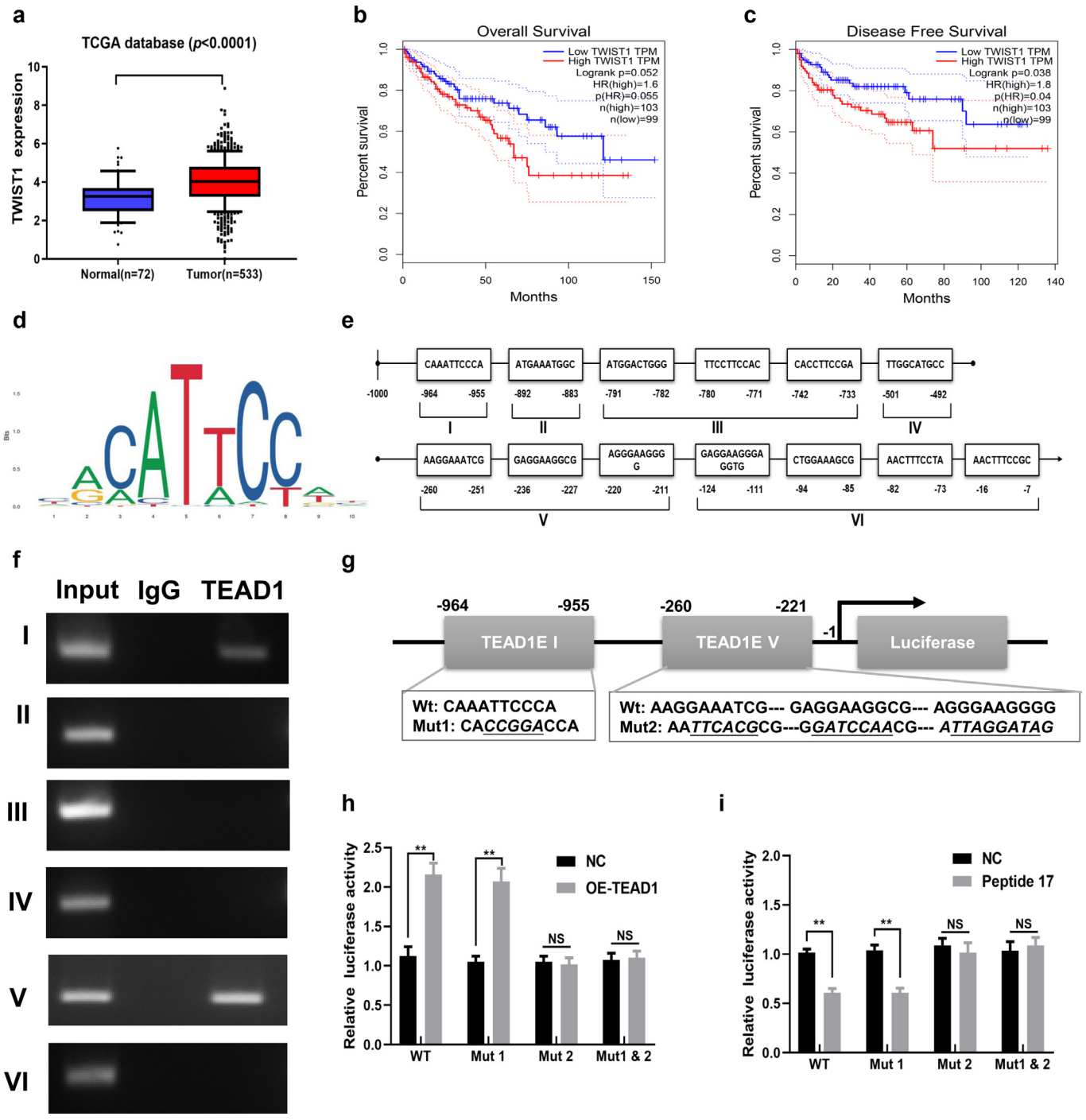

Fig. 8. TEAD1 promoted EMT by transcriptional up-regulation TWIST1. a. TCGA cohort analysis of the Twist1 expression in ccRCC tumor samples and pair-matched normal tissues. **b-c.** Kaplan–Meier analysis indicated that higher level of Twist1 expression was associated with worse overall survival(**b**) and disease-free survival(**c**). **d.** TEAD1 response element motif sequences. **e.** Bioinformatics analysis of potential TEAD1-binding sites in 1 kb of Twist1 promoter region using Jaspar database. **f.** ChIP assays showing that TEAD1 can bind to potential binding sites in the Twist1 promoter. **g.** Diagram of TEAD1E I-mut and TEAD1E V- mut in the Twist1 promoter. **h-i.** Co-transfection of TEAD1E wildtype or mutant in Twist1 promoter pGL3-Luciferase constructs, then into A498 cells with/without TEAD1(**h**), and into 786-O cells with/without Peptide 17(**i**). The luciferase assay was applied to detect the promoter activity. $^{**}P<0.01$, NS-not significant compared to the controls. The n values indicate the number of patients. Data are given as mean ± SD, N.S, not significant, $^{*}P < 0.05$, $^{**}P < 0.01$(Student's *t*-test).

elements (TEAD1Es) within proximal 1Kb promoter region (Fig. 8d), and found six putative TEAD1Es (Fig. 8e). ChIP assay revealed that TEAD1 could bind to TEAD1E I and TEAD1E V, but not TEAD1E II, III, IV or VI (Fig. 8f). Then, we cloned this 1 kb SH3BGRL2 promoter into pGL3-basic luciferase reporter vector (Fig. 8g). The results revealed that OE-TEAD1 significantly increased the wild-type and Mut1 group promoter luciferase reporter activity, but no change was observed in Mut2 group or Mut1&2 group (Fig. 8h). In contrast, adding Peptide 17 could decrease the luciferase reporter activity (Fig. 8i), suggesting TEAD1 modulated the Twist1 expression via binding to its promoter.

To investigate the clinical correlation between SH3BGRL2, hippo pathway and Twist1, immunohistochemical staining (IHC) were tested in ccRCC and adjacent normal tissues (Fig. 9a). We found that SH3BGRL2, LATS1/2 and P-YAP tended to have higher expression in normal tissues, while the expression of the TEAD1 and Twist1 were higher in ccRCC samples (Fig. 9b). Pairwise correlation showed

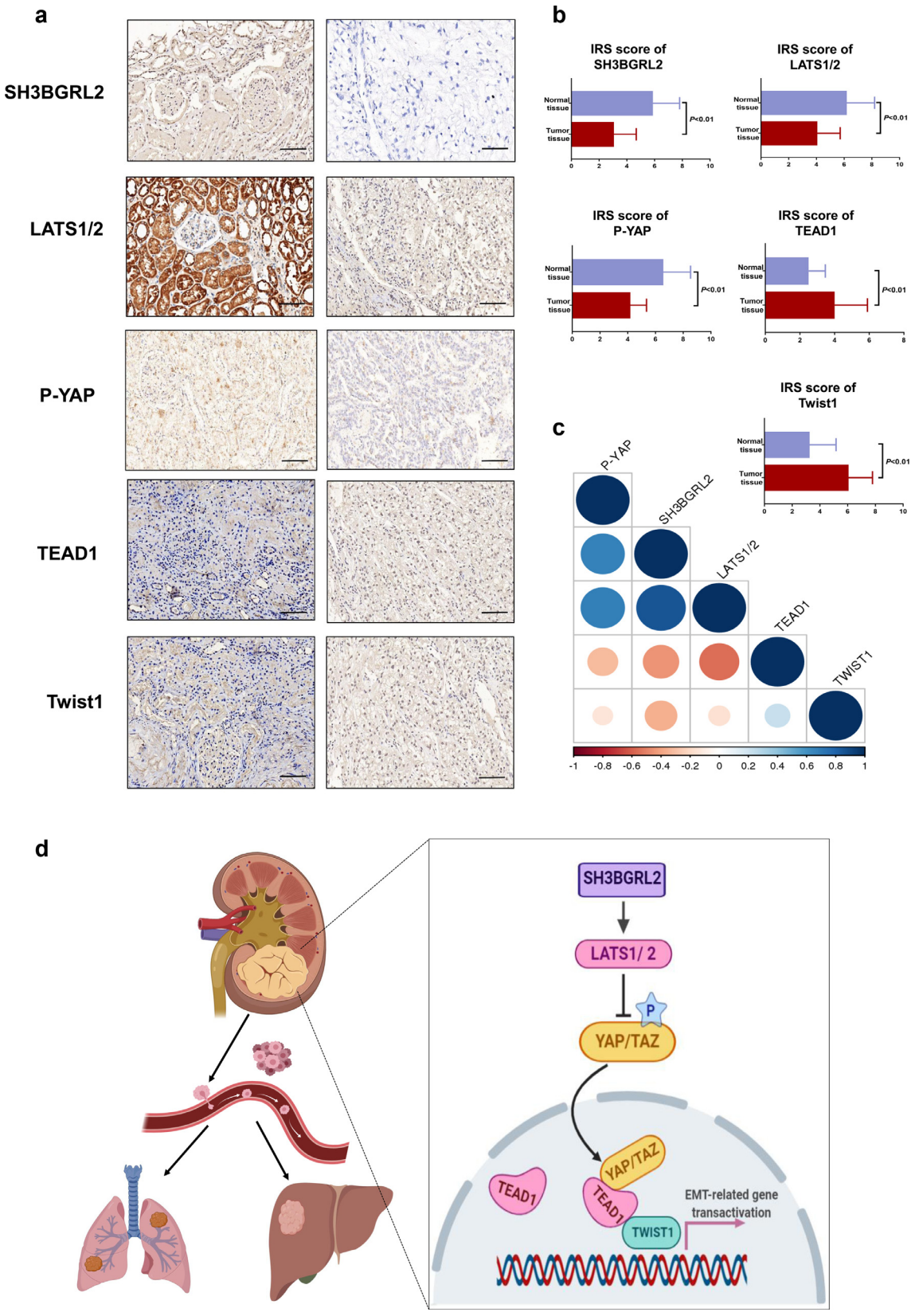

Fig. 9. Associations of SH3BGRL2 expression with Hippo signaling and Twist1 in ccRCC. a. Representative images of IHC staining for SH3BGRL2, LATS1/2, P-YAP, TEAD1 and Twist1 in ccRCC tissues and paired normal tissues. **b.** The IHC score of SH3BGRL2, LATS1/2, P-YAP, TEAD1 and Twist1 in ccRCC tissues and paired normal tissues(n = 16), Data are given as mean ± SD, (Student's t-test). **c.** Pairwise Spearman rank correlation among SH3BGRL2, LATS1/2, P-YAP, TEAD1 and Twist1 expression. Blue indicates positive and red negative correlation as reflected by the color legend below. **d.** Schematic representation for the mechanism of SH3BGRL2/Hippo-TEAD1 axis as a switch that regulates EMT in human ccRCC progression and metastasis by targeting Twist1 network.

SH3BGRL2 was positively correlated with LATS1/2, P-YAP, and was negatively correlated with TEAD1 and Twist1(Fig. 9c).

4. Discussion

Tumor metastasis leads to a poor prognosis for patients with ccRCC, but the mechanisms are largely unknown. Accumulating evidence indicates that SH3BGRL2 might play critical roles in the initiation and progression of human cancers [15, 40, 41]. However, the biological function and molecular mechanisms of SH3BGRL2 in ccRCC still elusive. In this study, we firstly reported that SH3BGRL2 was downregulated in ccRCC tumor, especially in metastatic tissue, and was associated with poor clinical prognosis. Moreover, overexpression or knockdown SH3BGRL2 could suppress or promote ccRCC cells proliferation and metastasis both in vitro and in vivo. Mechanically, SH3BGRL2 activated Hippo-TEAD1signaling and suppressed the transcription of Twist1 to intermediate ccRCC cells metastasis.

SH3BGRL2, located on chromosome 6q13-15 [5], contains four exons and three introns spread over 72 Kb of genomic DNA. This genomic region is associated with several solid tumors, such as prostate cancer [42], hepatocellular carcinoma [43] and breast cancer [44]. Previous studies showed that SH3BGRL2 was downregulated in esophageal squamous cell carcinoma [14], anaplastic thyroid carcinoma [45], ovarian chemotherapy resistance cells [15] and endometrial stromal cells [46]. Our study also found SH3BGRL2 was down-expression in ccRCC tumor than adjacent normal tissues. Clinically, the level of SH3BGRL2 in tumor tissues of ccRCC patients with metastasis or recurrence were lower than those of patients without, and downregulation of SH3BGRL2 significantly correlated with adverse pathological and clinical features. In addition, Kaplan-Meier survival curves showed that ccRCC patients with lower SH3BGRL2 expression had poorer overall survival and disease-free survival. Furthermore, the effects of SH3BGRL2 on tumor growth and metastasis were directly shown in our in vitro and in vivo studies. These clinical and experimental evidences suggested that SH3BGRL2 could be involved in ccRCC progression and metastasis and could be used as an independent prognostic marker for patients with ccRCC.

The reason for the decrease of SH3BGRL2 expression in ccRCC remains unclear. As we all known, most of ccRCC are associated with loss of von Hippel-Lindau tumor suppressor (VHL) function and deregulation of hypoxia (HIF) pathways [47, 48]. Considering SH3BGRL2 contains two protein binding domains, a Src homology 3 (SH3) and an ENA/VASP Homology 1 (EVH1) domain [5]. We hypothesis that HIF and/or VHL might interacted with these two domains. Interestingly, previous study reported HIF could regulated VHL-PTP1B-Src signaling axis in metastatic RCC [49].Tang et al. also found HIF-1α acted at downstream of TNF-α to inhibit VASP expression and to modulate the acute pulmonary inflammation process [50]. But the detailed relationship of HIF-VHL and SH3BGRL2, needs to be further studied.

Accumulating studies suggests that Epithelial-Mesenchymal Transition (EMT) plays an important role in tumor invasion and metastasis [29, 51]. However, the driving force of the EMT of ccRCC remains poorly understood. Through functional studies and bioinformatics analyses, our study found SH3BGRL2 target multiple EMT related genes including ZO-1, E-cadherin, N-cadherin and Twist1, and inhibited the ccRCC EMT process. Twist1, a basic-helix-loop-helix transcription factor, is a key player in tumor metastasis by inducing EMT and promoting invadopodia-mediated extracellular matrix degradation [38, 52]. Previous studies found Twist1 could be as biomarker for prediction of poor prognosis in nasopharyngeal carcinoma [53], oral cancer [54] and esophageal squamous cell carcinoma [55]. Consistently, our study also found the levels of Twist1 in tumor tissues of ccRCC patients with metastasis were higher than those of patients without, and higher expression of Twist1 showed a significant correlation with advanced pathological and clinical stage. Kaplan-Meier survival curves showed that the higher expression of Twist1 correlated with poor patients' prognosis, suggesting a pivotal role of Twist1 in ccRCC progression and metastasis.

The Hippo signaling pathway is a highly conserved tumor suppressor pathway [56], including LATS 1/2, YAP and TEAD [57], in which YAP-TEAD induced transcriptional responses are essential in proliferation and metastasis of cancer cells [58, 59] . It has been reported that LATS1/2 has decreased expression in many solid tumors, such as hepatocellular carcinoma [60], breast cancer [61] and gastric cancer [62]. Our finding also demonstrated LATS1/2 was significantly suppressed in ccRCC metastasis tissues compared with primary tumor tissues. In addition, lower expression of LATS 1/2 indicated worse overall survival and disease free survival rate, but the mechanism by which the hippo pathway was still largely unknown. Our key finding was identified SH3BGRL2 as a novel regulator of the hippo pathway in ccRCC. The functional studies showed SH3BGRL2 could suppress ccRCC cell growth and metastasis through interacting with LATS1/2-YAP-TEAD1 axis. Through CHIP assay and luciferase report assay, we found that YAP1 contributed to EMT procession by transcriptionally activating the Twist1 expression via binding to TEAD1

In summary, our findings revealed that SH3BGRL2 expression was significantly decreased in ccRCC and correlated with poor prognosis of ccRCC patients. Mechanistically (Fig. 9d), SH3BGRL2 inhibited ccRCC growth and metastasis via activating Hippo-YAP/TEAD1 signaling pathway, then though transcriptionally downregulating Twist1 and shifting EMT progression. Collectively, our finding suggested that SH3BGRL2 might have considerable potential as a prognosis predictor and therapeutic target for ccRCC.

Declaration of Competing Interest

The authors declare no conflicts of interest.

Acknowledgements

This study was supported by the National Natural Science Foundation of China (No. 31670772, 81870517, 81500534 and 81903113). The National Research Foundation for the Doctoral Program of Higher Education of China (No. 20130142120072), and Innovation Foundation of Huazhong University of Science and Technology (No. 1802030). The funders had no role in the design of the study, data collection, data analysis, interpretation, or the writing of this report.

Author contributions

B Peng and L Yin designed the experiments. L Yin executed the experiments. H Yang and L Yin drafted the manuscript. WJ Li assisted with animal breeding. KY Wang, H Shi, AM Xu assisted with clinical samples collection. RH Wang assisted the bioinformatics study. All authors participated in revising the manuscript and agreed to the final version.

Ethics approval and consent to participate

The tissue samples used for the study were conformed to the 1975 Declaration of Helsinki and was approved by the ethics committee of Shanghai Tenth People's Hospital, School of Medicine in Tongji University. Informed consent was obtained from all patients. All of the mice experiments were performed under protocols approved by the Institutional Animal Care and Use Committee of the Tongji University.

Funding

This study was supported by the National Natural Science Foundation of China.

Supplementary materials

Supplementary material associated with this article can be found in the online version at doi:10.1016/j.ebiom.2019.12.005.

References

[1] Siegel RL, Miller KD, Jemal A. Cancer statistics, 2019. CA Cancer J Clin 2019;69(1):7–34.
[2] Barata PC, Rini BI. Treatment of renal cell carcinoma: current status and future directions. CA Cancer J Clin 2017;67(6):507–24.
[3] Rini BI, Campbell SC, Escudier B. Renal cell carcinoma. Lancet 2009;373(9669):1119–32.
[4] Eggener SE, Yossepowitch O, Pettus JA, Snyder ME, Motzer RJ, Russo P. Renal cell carcinoma recurrence after nephrectomy for localized disease: predicting survival from time of recurrence. J Clin Oncol 2006;24(19):3101–6.
[5] Mazzocco M, Maffei M, Egeo A, Vergano A, Arrigo P, Di Lisi R, et al. The identification of a novel human homologue of the SH3 binding glutamic acid-rich (SH3BGR) gene establishes a new family of highly conserved small proteins related to thioredoxin superfamily. Gene 2002;291(1−2):233–9.
[6] Tong F, Zhang M, Guo X, Shi H, Li L, Guan W, et al. Expression patterns of SH3BGR family members in zebrafish development. Dev Genes Evol 2016;226(4):287–95.
[7] Li W, Yan Q, Ding X, Shen C, Hu M, Zhu Y, et al. The SH3BGR/STAT3 pathway regulates cell migration and angiogenesis induced by a gammaherpesvirus microRNA. PLoS Pathog 2016;12(4):e1005605.
[8] Wang H, Liu B, Al-Aidaroos AQ, Shi H, Li L, Guo K, et al. Dual-faced SH3BGRL: oncogenic in mice, tumor suppressive in humans. Oncogene 2016;35(25):3303–13.
[9] Xu L, Zhang M, Li H, Guan W, Liu B, Liu F, et al. SH3BGRL as a novel prognostic biomarker is down-regulated in acute myeloid leukemia. Leuk Lymphoma 2018;59(4):918–30.
[10] Yin L, Gao S, Shi H, Wang K, Yang H, Peng B. TIP-B1 promotes kidney clear cell carcinoma growth and metastasis via EGFR/AKT signaling. Aging (Albany NY) 2019;11.
[11] Chiang CY, Pan CC, Chang HY, Lai MD, Tzai TS, Tsai YS, et al. SH3BGRL3 protein as a potential prognostic biomarker for urothelial carcinoma: a novel binding partner of epidermal growth factor receptor. Clin Cancer Res 2015;21(24):5601–11.
[12] Frame MC. Src in cancer: deregulation and consequences for cell behaviour. Biochim Biophys Acta 2002;1602(2):114–30.
[13] Krause M, Dent EW, Bear JE, Loureiro JJ, Gertler FB. Ena/VASP proteins: regulators of the actin cytoskeleton and cell migration. Annu Rev Cell Dev Biol 2003;19:541–64.
[14] Yang Y, Li D, Yang Y, Jiang G. An integrated analysis of the effects of microRNA and mRNA on esophageal squamous cell carcinoma. Mol Med Rep 2015;12(1):945–52.
[15] Ribeiro JR, Schorl C, Yano N, Romano N, Kim KK, Singh RK, et al. HE4 promotes collateral resistance to cisplatin and paclitaxel in ovarian cancer cells. J Ovarian Res 2016;9(1):28.
[16] Mo JS, Meng Z, Kim YC, Park HW, Hansen CG, Kim S, et al. Cellular energy stress induces AMPK-mediated regulation of YAP and the Hippo pathway. Nat Cell Biol 2015;17(4):500–10.
[17] Yu M, Cui R, Huang Y, Luo Y, Qin S, Zhong M. Increased proton-sensing receptor GPR4 signalling promotes colorectal cancer progression by activating the hippo pathway. EBioMedicine 2019;48:264–76.
[18] Shi X, Liu Z, Liu Z, Feng X, Hua F, Hu X, et al. Long noncoding rna PCAT6 functions as an oncogene by binding to EZH2 and suppressing LATS2 in non-small-cell lung cancer. EBioMedicine 2018;37:177–87.
[19] Yin L, Li W, Wang G, Shi H, Wang K, Yang H, et al. NR1B2 suppress kidney renal clear cell carcinoma (KIRC) progression by regulation of LATS 1/2-YAP signaling. J Exp Clin Cancer Res 2019;38(1):343.
[20] Zhang X, Zhao H, Li Y, Xia D, Yang L, Ma Y, et al. The role of YAP/TAZ activity in cancer metabolic reprogramming. Mol Cancer 2018;17(1):134.
[21] Xu S, Zhang H, Chong Y, Guan B, Guo P. YAP promotes VEGFA expression and tumor angiogenesis though Gli2 in human renal cell carcinoma. Arch Med Res 2019;50(4):225–33.
[22] Sun J, Wang X, Tang B, Liu H, Zhang M, Wang Y, et al. A tightly controlled Src-YAP signaling axis determines therapeutic response to dasatinib in renal cell carcinoma. Theranostics 2018;8(12):3256–67.
[23] Huang T, Wang G, Hu Y, Shi H, Wang K, Yin L, et al. Structural and functional abnormalities of penile cavernous endothelial cells result in erectile dysfunction at experimental autoimmune prostatitis rat. J Inflamm (Lond) 2019;16:20.
[24] Bi J, Liu H, Cai Z, Dong W, Jiang N, Yang M, et al. Circ-BPTF promotes bladder cancer progression and recurrence through the miR-31-5p/RAB27A axis. Aging (Albany NY) 2018;10(8):1964–76.
[25] Sauter G, Simon R, Hillan K. Tissue microarrays in drug discovery. Nat Rev Drug Discov 2003;2(12):962–72.
[26] Ma XL, Shen MN, Hu B, Wang BL, Yang WJ, Lv LH, et al. CD73 promotes hepatocellular carcinoma progression and metastasis via activating PI3K/AKT signaling by inducing Rap1-Mediated membrane localization of P110beta and predicts poor prognosis. J Hematol Oncol 2019;12(1):37.
[27] Carey MF, Peterson CL, Smale ST. Chromatin immunoprecipitation (ChIP). Cold Spring Harb Protoc 2009;2009(9) pdb prot5279.
[28] Brooks SA, Brannon AR, Parker JS, Fisher JC, Sen O, Kattan MW, et al. ClearCode34: a prognostic risk predictor for localized clear cell renal cell carcinoma. Eur Urol 2014;66(1):77–84.
[29] Pastushenko I, Brisebarre A, Sifrim A, Fioramonti M, Revenco T, Boumahdi S, et al. Identification of the tumour transition states occurring during EMT. Nature 2018;556(7702):463–8.
[30] Zheng X, Carstens JL, Kim J, Scheible M, Kaye J, Sugimoto H, et al. Epithelial-to-mesenchymal transition is dispensable for metastasis but induces chemoresistance in pancreatic cancer. Nature 2015;527(7579):525–30.
[31] Thompson BJ, Cohen SM. The Hippo pathway regulates the bantam microRNA to control cell proliferation and apoptosis in Drosophila. Cell 2006;126(4):767–74.
[32] Yu FX, Zhao B, Guan KL. Hippo pathway in organ size control, tissue homeostasis, and cancer. Cell 2015;163(4):811–28.
[33] Warde-Farley D, Donaldson SL, Comes O, Zuberi K, Badrawi R, Chao P, et al. The Genemania prediction server: biological network integration for gene prioritization and predicting gene function. Nucleic Acids Res 2010;38(Web Server issue):W214–20.
[34] Zhang Z, Lin Z, Zhou Z, Shen HC, Yan SF, Mayweg AV, et al. Structure-Based design and synthesis of potent cyclic peptides inhibiting the YAP-Tead protein-protein interaction. ACS Med Chem Lett 2014;5(9):993–8.
[35] Yu MH, Zhang W. TEAD1 enhances proliferation via activating SP1 in colorectal cancer. Biomed Pharmacother 2016;83:496–501.
[36] Tome-Garcia J, Erfani P, Nudelman G, Tsankov AM, Katsyv I, Tejero R, et al. Analysis of chromatin accessibility uncovers TEAD1 as a regulator of migration in human glioblastoma. Nat Commun 2018;9(1):4020.
[37] Wen T, Liu J, He X, Dong K, Hu G, Yu L, et al. Transcription factor TEAD1 is essential for vascular development by promoting vascular smooth muscle differentiation. Cell Death Differ 2019.
[38] Yang J, Mani SA, Donaher JL, Ramaswamy S, Itzykson RA, Come C, et al. Twist, a master regulator of morphogenesis, plays an essential role in tumor metastasis. Cell 2004;117(7):927–39.
[39] Khan A, Fornes O, Stigliani A, Gheorghe M, Castro-Mondragon JA, van der Lee R, et al. JASPAR 2018: update of the open-access database of transcription factor binding profiles and its web framework. Nucleic Acids Res 2018;46(D1):D1284.
[40] Lee CH, Kuo WH, Lin CC, Oyang YJ, Huang HC, Juan HF. MicroRNA-regulated protein-protein interaction networks and their functions in breast cancer. Int J Mol Sci 2013;14(6):11560–606.
[41] Zhou RS, Zhang EX, Sun QF, Ye ZJ, Liu JW, Zhou DH, et al. Integrated analysis of lncRNA-miRNA-mRNA ceRNA network in squamous cell carcinoma of tongue. BMC Cancer 2019;19(1):779.
[42] Rokman A, Koivisto PA, Matikainen MP, Kuukasjarvi T, Poutiainen M, Helin HJ, et al. Genetic changes in familial prostate cancer by comparative genomic hybridization. Prostate 2001;46(3):233–9.
[43] Sakakura C, Hagiwara A, Taniguchi H, Yamaguchi T, Yamagishi H, Takahashi T, et al. Chromosomal aberrations in human hepatocellular carcinomas associated with hepatitis C virus infection detected by comparative genomic hybridization. Br J Cancer 1999;80(12):2034–9.
[44] Rodriguez C, Causse A, Ursule E, Theillet C. At least five regions of imbalance on 6q in breast tumors, combining losses and gains. Genes Chromosomes Cancer 2000;27(1):76–84.
[45] Weinberger P, Ponny SR, Xu H, Bai S, Smallridge R, Copland J, et al. Cell cycle M-Phase genes are highly upregulated in anaplastic thyroid carcinoma. Thyroid 2017;27(2):236–52.
[46] Mei J, Li MQ, Li DJ, Sun HX. MicroRNA expression profiles and networks in CXCL12stimulated human endometrial stromal cells. Mol Med Rep 2017;15(1):249–55.
[47] Schodel J, Grampp S, Maher ER, Moch H, Ratcliffe PJ, Russo P, et al. Hypoxia, hypoxia-inducible transcription factors, and renal cancer. Eur Urol 2016;69(4):646–57.
[48] Hsieh JJ, Purdue MP, Signoretti S, Swanton C, Albiges L, Schmidinger M, et al. Renal cell carcinoma. Nat Rev Dis Primers 2017;3:17009.
[49] Suwaki N, Vanhecke E, Atkins KM, Graf M, Swabey K, Huang P, et al. A HIF-regulated VHL-PTP1B-Src signaling axis identifies a therapeutic target in renal cell carcinoma. Sci Transl Med 2011;3(85) 85ra47.
[50] Tang M, Tian Y, Li D, Lv J, Li Q, Kuang C, et al. TNF-alpha mediated increase of HIF-1alpha inhibits VASP expression, which reduces alveolar-capillary barrier function during acute lung injury (ALI). PLoS ONE 2014;9(7):e102967.
[51] Wicki A, Lehembre F, Wick N, Hantusch B, Kerjaschki D, Christofori G. Tumor invasion in the absence of epithelial-mesenchymal transition: podoplanin-mediated remodeling of the actin cytoskeleton. Cancer Cell 2006;9(4):261–72.
[52] Eckert MA, Lwin TM, Chang AT, Kim J, Danis E, Ohno-Machado L, et al. Twist1-induced invadopodia formation promotes tumor metastasis. Cancer Cell 2011;19(3):372–86.
[53] Zhuo X, Chang A, Huang C, Yang L, Xiang Z, Zhou Y. Expression of TWIST, an inducer of epithelial-mesenchymal transition, in nasopharyngeal carcinoma and its clinical significance. Int J Clin Exp Pathol 2014;7(12):8862–8.
[54] da Silva SD, Alaoui-Jamali MA, Soares FA, Carraro DM, Brentani HP, Hier M, et al. TWIST1 is a molecular marker for a poor prognosis in oral cancer and represents a potential therapeutic target. Cancer 2014;120(3):352–62.
[55] Lee KW, Sung CO, Kim JH, Kang M, Yoo HY, Kim HH, et al. CD10 expression is enhanced by Twist1 and associated with poor prognosis in esophageal squamous cell carcinoma with facilitating tumorigenicity in vitro and in vivo. Int J Cancer 2015;136(2):310–21.
[56] Zhang J, Ji JY, Yu M, Overholtzer M, Smolen GA, Wang R, et al. YAP-dependent induction of amphiregulin identifies a non-cell-autonomous component of the Hippo pathway. Nat Cell Biol 2009;11(12):1444–50.
[57] Moroishi T, Park HW, Qin B, Chen Q, Meng Z, Plouffe SW, et al. A YAP/TAZ-induced feedback mechanism regulates Hippo pathway homeostasis. Genes Dev 2015;29(12):1271–84.

[58] Marti P, Stein C, Blumer T, Abraham Y, Dill MT, Pikiolek M, et al. YAP promotes proliferation, chemoresistance, and angiogenesis in human cholangiocarcinoma through TEAD transcription factors. Hepatology 2015;62(5):1497–510.
[59] Kim T, Hwang D, Lee D, Kim JH, Kim SY, Lim DS. MRTF potentiates TEAD-YAP transcriptional activity causing metastasis. EMBO J 2017;36(4):520–35.
[60] Britschgi A, Duss S, Kim S, Couto JP, Brinkhaus H, Koren S, et al. The Hippo kinases LATS1 and 2 control human breast cell fate via crosstalk with ERalpha. Nature 2017;541(7638):541–5.
[61] Yi J, Lu L, Yanger K, Wang W, Sohn BH, Stanger BZ, et al. Large tumor suppressor homologs 1 and 2 regulate mouse liver progenitor cell proliferation and maturation through antagonism of the coactivators YAP and TAZ. Hepatology 2016;64(5):1757–72.
[62] Zhang J, Wang G, Chu SJ, Zhu JS, Zhang R, Lu WW, et al. Loss of large tumor suppressor 1 promotes growth and metastasis of gastric cancer cells through upregulation of the YAP signaling. Oncotarget 2016;7(13):16180–93.